Longitudinal Single-Bunch Instability in the ILC Damping Rings: Estimate of Current Threshold

Marco Venturini*
Lawrence Berkeley National Laboratory, University of California, Berkeley, California, 94720
(Dated: June 25, 2008)

Characterization of single-bunch instabilities in the International Linear Collider (ILC) damping rings (DRs) has been indicated as a high-priority activity toward completion of an engineering design. In this paper we report on a first estimate of the current thresholds for the instability using numerical and analytical models of the wake potentials associated with the various machine components. The numerical models were derived (upon appropriate scaling) from designs of the corresponding components installed in existing machines. The current thresholds for instabilities were determined by numerical solution of the Vlasov equation for the longitudinal dynamics. For the DR baseline lattice as of Feb. 2007 we find the critical current for instability to be safely above the design specifications leaving room for further optimization of the choice of the momentum compaction.

PACS numbers: 29.27.Bd, 41.60.Ap

I. INTRODUCTION

In order for the International Linear Collider (ILC) to meet the luminosity goal it is essential that properly damped and stable bunches be extracted from the damping rings (DRs). Past experience has taught that instabilities affecting the longitudinal phase space of beams exiting the DRs can result into significant beam quality degradation along the linac. Although a weak instability could perhaps be tolerated, as was the case for the SLC damping rings after replacement of the original vacuum chamber, a desirable approach is to seek to avoid conditions for longitudinal single-bunch instabilities altogether. Characterization of these instabilities, therefore, is critical and indeed has been indicated as a high-priority item in the R&D agenda toward completion of the Engineering Design Report (EDR) as it carries implications regarding specification of the machine components and choice of the lattice parameters.

There are two aspects to this activity: modelling of the relevant sources of the impedance and study of the beam dynamics based on that modelling. The accuracy of the instability estimates depends on that of the impedance modelling, which in turn would require detailed designs of the most significant machine components. A complete technical design of these components is not expected to become available until the end of the work period for the EDR. Some estimate, albeit approximate, of the instability threshold is however desirable while the DR design is being finalized and can provide useful guidance toward the selection of a workable set of machine parameters. To this end we have initiated a study to characterize the longitudinal single-bunch instability based on approximate models of relevant impedance sources derived from the design of components in existing machines (suitably scaled to meet the DRs basic requirements).

In this report we summarize the results of studies that were completed as of Dec. 2007 [9] making use of numerical models of impedances for the rf cavities and the beam position monitors (BPMs) and analytical models for resistive wall (RW), which are believed to represent the main contributors to the total impedance. We calculated the current thresholds associated with these models for the current DR baseline lattice using a Vlasov solver we have developed specifically for the study of longitudinal dynamics in beams. A preliminary report of our studies was presented in [1].

Our results show that the estimated current thresholds are abundantly above the machine design current and suggest that there is latitude for optimizing the choice of the basic lattice design parameters. In particular, it appears that a conservatively specified large momentum compaction could stand a significant reduction without compromising the stability of longitudinal dynamics.

The content of the paper is as follows. After reviewing the basic equations of motion for the longitudinal dynamics in Sec. II, we present the impedance models and report on the calculation of the instability thresholds in Sec. III. In Sec.'s IV and V we compare the more accurate calculation of the instability thresholds determined using the Vlasov solver to a rough estimate based on the Keil-Schnell-Boussard criterion (or Boussard criterion, for short) providing a context to interpret erroneous early estimates that during the the lattice configuration studies [2] had indicated the possibility of an alarmingly large instability.

* mventurini@lbl.gov

TABLE I: Relevant Parameters for the ILC DRs – Feb. 2007 Baseline Design

Description	Notation	Value
Energy	E_0	5.0 GeV
Ring circumference	C	6695.057 m
Pipe radius (except wiggler sections)	b_a	2.5 cm
Pipe radius in wiggler sections	b_w	2.3 cm
Conductivity of pipe (Al)	σ	$3.5 \times 10^7\ \Omega^{-1}\mathrm{m}^{-1}$
Momentum compaction	α	4.2×10^{-4}
Synchrotron tune	ν_s	0.064
Natural bunch length	σ_{z0}	9.0 mm
Natural rms relative energy spread	$\sigma_{\delta 0}$	1.28×10^{-3}
Longitudinal damping time	τ_d	12.9 ms
Harmonic number	h_n	14516
rf voltage	$\hat{V}_{\mathrm{rf}}$	24 MV
rf phase	ϕ_s	151 deg
rf frequency	$\omega_{\mathrm{rf}}/2\pi$	650 MHz
Number of cavities		18
Total length of wiggler straights	L_w	300 m
Bunch population	N	2×10^{10}

II. EQUATIONS OF MOTION

The longitudinal motion is described by the coordinates z, the position with respect to the synchronous particle, and $\Delta E/E_0 = (E - E_0)/E_0$ the relative deviation from the design energy. Denote with T_0 the revolution time for an on-energy particle, C the ring circumference, β_0 the relativistic factor ($c\beta_0 = C/T_0$), and $\eta = \alpha - 1/\gamma_0^2$ the slippage factor, where α is the momentum compaction and γ_0 the relativistic factor. The equations of motion then read

$$\frac{dz}{dt} = -\frac{c\eta}{\beta_0}\frac{\Delta E}{E_0}, \tag{1}$$

$$\frac{d}{dt}\left(\frac{\Delta E}{E_0}\right) = -\frac{eV(z)}{T_0 E_0}, \tag{2}$$

where $V(z) = V_{\mathrm{rf}}(z) + V_c(z)$ is the voltage difference experienced by a particle through one machine revolution. The term $V_{\mathrm{rf}}(z)$ represents the contribution from the rf cavities. In linear approximation

$$V_{\mathrm{rf}}(z) = -z\frac{h_n}{R}\hat{V}_{\mathrm{rf}}\cos\phi_s, \tag{3}$$

where $\hat{V}_{\mathrm{rf}}$ is the peak rf-voltage, ϕ_s the synchronous phase, $h_n = \omega_{\mathrm{rf}}/\omega_0$ the harmonic number, and R the ring average radius. At small currents only V_{rf} contributes to the voltage. Combining (1), (2), and (3) yields $\ddot{z} = -\omega_s^2 z$, with the synchrotron frequency $\omega_s^2 = \omega_0^2(eh_n\hat{V}_{\mathrm{rf}}|\eta\cos\phi_s|/2\pi E_0\beta_0^2)$, where $\omega_0 = 2\pi/T_0$ is the revolution frequency.

Collective effects are described by a beam induced voltage V_c. The interaction between particles can occur directly through radiation or Coulomb forces, or can be mediated through the surrounding machine environment (wake fields). Either way, V_c can be modelled in terms of a "wake potential" function $W(z - z')$

$$V_c(z) = -eN\int W(z - z')\rho(z')dz', \tag{4}$$

where N is the number of particles per bunch and $\rho(z)$ the longitudinal density with normalization $\int \rho(z)dz = 1$. $W(z - z')/C$ has the meaning of longitudinal electric field per unit charge (averaged along the ring circumference C) at point z due to a unit charge located at point z', *i.e.* $W(z - z')$ has dimensions of voltage over charge; in this paper we set the sign of $W(z - z')$ by the convention that a positive value corresponds to energy gain (this is opposite of Chao's definition [3], where a positive sign corresponds to energy loss).

The frequency-domain companion of the wake potential is the impedance defined as

$$Z(k) = -\frac{1}{c\beta_0}\int_{-\infty}^{\infty} dz W(z)e^{-ikz}. \tag{5}$$

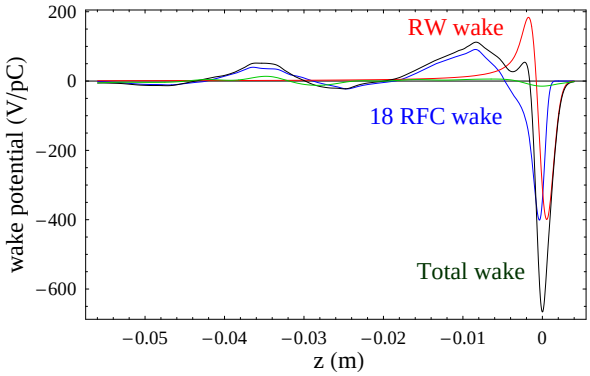

FIG. 1: Wake potential for resistive wall (red curve), the 18 rf cavities (blue curve), 908BPMS (green curve), and their sum (black curve).

Conversely

$$W(z) = -\frac{c\beta_0}{2\pi}\int_{-\infty}^{\infty} dk e^{ikz} Z(k). \tag{6}$$

Introduce the scaled coordinates $q = z/\sigma_{z0}$ and $p = -(\Delta E/E_0)/\sigma_{\delta 0}$, where σ_{z0} and $\sigma_{\delta 0}$ are the rms beam length and relative energy spread at equilibrium at low current. At equilibrium $\sigma_{\delta 0}$ and σ_{z0} are related by $\nu_s\beta_0(\sigma_{z0}/R) = |\eta|\sigma_{\delta 0}$ where $\nu_s = \omega_s/\omega_0$ is the synchrotron tune. Using the scaled time $\tau = \omega_s t$ as the independent variable the equations of motion can be rewritten as

$$\frac{dq}{d\tau} = p, \tag{7}$$

$$\frac{dq}{d\tau} = -q + I_c F(q, \tilde{\rho}(q)), \tag{8}$$

where we have introduced the current parameter

$$I_c = \frac{e^2 N}{2\pi\nu_s E_0 \sigma_{\delta 0}}, \tag{9}$$

and written the collective force contribution as

$$F(q, \tilde{\rho}(q)) = -\int_{-\infty}^{\infty} \tilde{W}(q - q')\tilde{\rho}(q')dq', \tag{10}$$

where $\tilde{W}(q) = W(z/\sigma_{z0})$ and $\tilde{\rho}(q) = \rho(z/\sigma_{z0})\sigma_{z0}$ are the wake function and bunch density expressed in terms of the scaled longitudinal distance q.

The beam distribution function $f(q, p)$ in phase space evolves according to the Vlasov-Fokker-Planck equation with the Vlasov part (LHS of equation) accounting for rf focusing and collective effects and the Fokker-Planck part modelling radiation damping and quantum excitations:

$$\frac{\partial f}{\partial \tau} + \frac{\partial f}{\partial q}p + \frac{\partial f}{\partial p}\left[-q + I_c F(q, f, \tau)\right] = \frac{2}{\omega_s \tau_d}\frac{\partial}{\partial p}\left(pf + \frac{\partial f}{\partial p}\right), \tag{11}$$

where τ_d is the longitudinal damping time. We are interested in determining stability of equilibrium beam distributions that are solutions of (11). Eq. (11) admits equilibria in the form $f_0(q, p) = \tilde{\rho}_0(q)\exp(-p^2/2)/\sqrt{2\pi}$ (Haïssinski solutions) with $\tilde{\rho}_0(q)$ satisfying the Haïssinski equation $\tilde{\rho}_0' = (-q + I_c F)\tilde{\rho}_0$.

In the following we will investigate stability by solving numerically (11) using the methods described in [5] starting from a Haïssinski distribution. In the present analysis we will neglect the Fokker-Planck part of the equation.

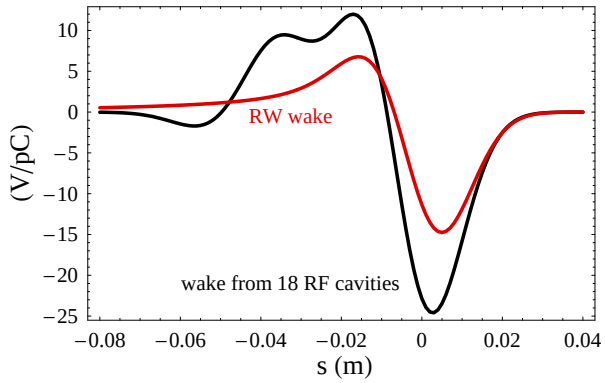

FIG. 2: Wake from resistive wall and rf cavities convoluted with the nominal $\sigma_{z0} = 9$ mm bunch.

III. IMPEDANCE MODELS AND CALCULATION OF INSTABILITY THRESHOLDS

A. Impedance Models

We have considered three distinct models of short-range wake potentials of increasing level of completeness.

- The first model consists of the wake potential due to the rf cavities only. These are expected to be the single largest source of impedance for the damping rings. The current design for the DRs calls for installation of 18 superconducting cavities at 650 MHz, a convenient harmonic of the 1.3 GHz frequency of the main linac rf structures. Examples of installed superconductng rf cavities in colliders are at KEKB and at Cornell CESR. Because both sets of cavities operate in the neighborhood of 500 MHz frequency and have tapers connecting to beam pipes with aperture different from that of the DRs, their design is not immediately usable for our purposes and requires some scaling to match both the 2.5 cm DR pipe radius at the end of the tapers and the design frequency. For our study we adopted the CESR cavity model. The wake functions for the cavities were determined by evaluating the longitudinal electric field driven by a finite size (0.5-mm rms gaussian) rigid charge source using a 2D numerical model [7]. Because of the finite length of the driving source used in the calculation causality is violated and the wake functions are non-zero for $z > 0$, see blue curve in Fig. 1. Notice that in our study we did not attempt to restore causality by artificially removing (or moving) the $z > 0$ part of the wake, as is sometimes done.

- The second model of wake potential consists of the sum of the contribution from the rf cavities and the resistive wall effect from the vacuum chamber. Resistive-wall effects were modelled using an analytical formula [3] valid for an infinitely long, straight vacuum chamber with circular cross section of radius b. Specifically, the longitudinal electric field caused by the finite conductivity of the pipe wall at $z < 0$ due to a charge e at $z = 0$ is given by

$$E_z^{rw}(z,b) = -\frac{4Z_0 ce}{\pi b^2}\left(\frac{1}{3}e^u\cos(\sqrt{3}u) - \frac{\sqrt{2}}{\pi}\int_0^\infty \frac{x^2 e^{ux^2}}{x^6+8}dx\right), \quad \text{for } z \le 0, \tag{12}$$

  with $u = z/(2\chi)^{1/3}b$ and $\chi = 1/Z_0\sigma b$ where σ is the conductivity of the vacuum chamber. For Aluminum at room temperature $\sigma = 3.5\times 10^7\ \Omega^{-1}\mathrm{m}^{-1}$. We distinguish between the wiggler sections (where the pipe radius is b_w) and the rest of the machine (with pipe radius b_a) and for $z < 0$ write the wake function for the resistive wall as:

$$W^{rw}(z) = L_w E_z^{rw}(z,b_w)/e + (C - L_w)E_z^{rw}(z,b_a)/e, \tag{13}$$

  (obviously $W(z) = 0$ for $z > 0$). However, we did not use directly (13) in our calculation. Instead, we first carried out a convolution with a 1-mm rms gaussian source in analogy with the way the wake functions for the other components of the vacuum chamber were determined. The plot of the RW wake so calculated is reported in Fig. 1 as the red curve. In Fig. 2 we report the profile of the same wake convoluted with a 9 mm gaussian bunch (red curve) an by comparison the convolution of the rf cavities wake with the same 9 mm bunch.

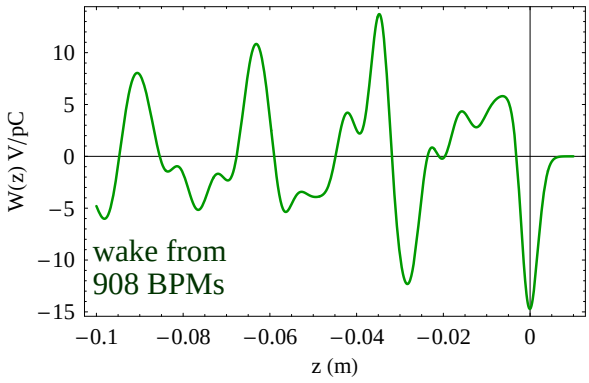

FIG. 3: Longitudinal wake potential contributed by 908 BPMs.

- Finally, the third model includes the contribution from 908 BPMs in addition to the wake potentials from the rf cavities and the resistive wall. For the BPMs, we took as a model the design of the devices installed in PEP-II. The PEP-II BPMs have four buttons of diameter 1.5 cm located on the wall of a 4.8 cm radius beampipe. In our adaptation to the DRs the button diameter was scaled to 0.8 cm and the beam pipe radius to $b_a = 2.5$ cm. Similarly to the rf cavities the wake potential for the BPMs was determined numerically by solving for the electromagnetic fields induced by a rigid gaussian source, in this case 1mm long (rms). A 3D field solver was used for the BPMs (whereas exploitation of the azimuthal symmetry in the design allowed for use of a faster 2D code for modelling of the rf cavities). The number of BPMs used in our study was chosen somewhat arbitrarily and set equal to the number of quadrupoles in the lattice. The wakefield is shown in Fig. 3. The picture shows a long tail resulting from the excitations of resonances with long time effects. The long tail is not of concern for single bunch effects but it is likely to require careful investigation toward future optimization of the BPM design in order to minimize the impact on coupled-bunch instabilities.

B. Current Threshold for Instability

In studying stability with the Vlasov solver we start from an equilibrium (Haïssinski solution). Above the instability threshold we expect that small deviations from equilibrium result into an exponential growth, as predicted from linear theory. In practice we found that the unavoidable small errors in the numerical determination of the equilibrium density suffices to seed the instability. To determine the growth rate we follow the evolution of the second or third moment of the energy density and fit an exponential curve against their envelope. The results of the growth rate calculations are plotted in Fig. 4 for the three impedance models described above. The instability threshold is defined by the intersection of the growth rate curves with the Im $\omega = 0$ axis. Because we are neglecting radiation damping this slightly underestimates the threshold for instability (the damping rate for the longitudinal motion is $1/\tau_d = 0.077$ msec^{-1}). Notice the generally non-monotonic dependence of the growth rates on the bunch population. In particular, or the impedance model accounting for the rf cavities and resistive wall (red curve in Fig. 4) this dependence results into an 'island of stability' between $N = 140 \times 10^{10}$ and 155×10^{10} particles/bunch. This non-trivial dependence appears to be caused by the variation of the shape of the Haïssinski equilibrium with current. As the bunch population increases the potential well distortions will cause the equilibrium to become shallower countering the otherwise expected increase of the growth rates with current. In the stability analysis reported in [1] for the rf cavities + RW model of impedance we missed this island of instability and estimated the threshold to be in the neighborhood of $N = 150 \times 10^{10}$ part./bunch. In fact, Fig. 4 shows that for the rf cavities + RW model of impedance the critical bunch population for instability is rather in the neighborhood of $N = 120 \times 10^{10}$ part./bunch. In a way consistent with intuition the same figure shows that more complete impedance models yield estimates of lower current thresholds for instability. In particular, notice that adding the wake potential from the 908 BPMs resulted in a net erosion of stability of about 15%. This is in spite of the fact that the peak value of the total BPM contribution is less than 3% than the peak value of the total (rf + RW + BPM) wake. This confirms previous observations [4] that fine details in the shape of a wake potentials can have a significant impact on beam dynamics.

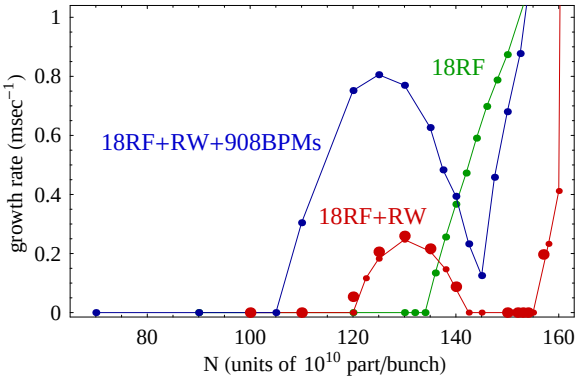

FIG. 4: Instability growth rates corresponding to the three models of impedance discussed in the text as function of the bunch population. The thresholds for instability as deduced from this figure are $N = 142$, 120 and 105×10^{10} part./bunch respectively for the impedance model including the rf cavities only (green data), rf cavities + resistive wall (red data), rf cavities + resistive wall + BPMs (blue data).

IV. BOUSSARD ANALYSIS

The Keil-Schnell-Boussard criterion is often used to give an analytical estimate of the instability thresholds. It can be stated in the form [10]

$$N_{\rm th} = \frac{Z_0}{[{\rm Z/n}]}\sqrt{\frac{\pi}{2}}\frac{\gamma\eta\sigma_{\delta 0}^2\sigma_{z0}}{r_e}, \tag{14}$$

where N_{th} is the critical bunch population for instability, $r_e = 2.82 \times 10^{-15}$ the classical electron radius, and [Z/n] is a real quantity (with dimensions of an impedance) related to the machine impedance. Generally the validity of the criterion is strictly dependent on the functional form of the impedance and form factor of the beam density.

For coasting beams $[{\rm Z/n}] = |Z(n)/n|$, where n is the harmonic number of the most unstable mode and $Z(n)$ the machine impedance. For bunched beams one has to provide some interpretation for the term[Z/n] . At least two prescriptions can be found in the literature. Assume a beam with gaussian density and rms width σ_{z0}.

The first prescription has the form:

$$\begin{aligned}[{\rm Z/n}] &= \frac{\sigma_{z0}}{R}\sum_{n=-\infty}^{\infty}\left|\frac{Z(n\omega_0)}{n}\right|e^{-(n\sigma_{z0}\omega_0/c)^2} \\ &\simeq \frac{\sigma_{z0}}{R}\int_{-\infty}^{\infty}\left|\frac{Z(k)}{k}\right|e^{-(k\sigma_{z0})^2}dk,\end{aligned} \tag{15}$$

where $\omega_0 = c/R$ is the revolution frequency and $n = \omega/\omega_0 = kR$.

The second interpretation postulates that $[Z/n] = |Z(k)/n|$, with n given by the mode $n = R/\sigma_z$ or $k = 1/\sigma_{z0}$.

According to the first interpretation, using in (15) the impedance for the wake potential from the 18 cavities we find [Z/n] = 46 mΩ, which gives a threshold $N_{\rm th} = 22 \times 10^{10}$, about factor 10 larger than the design value but more than a factor 6 smaller than the numerical calculation. The real and imaginary parts of the impedance for a single rf cavity are reported in Fig.'s 6 and 7.

V. BOUSSARD CRITERION FOR A RESONATOR MODEL OF IMPEDANCE

To get a sense of the accuracy of the Boussard estimates (or lack thereof) we consider a simplified model of impedance (that of a broadband resonator) and make a comparison between the instability thresholds as predicted by the above formulations of the Boussard criterion and that calculated numerically by solving the Vlasov equation.

The broadband resonator model [3] is defined by the impedance

$$Z_{\rm res}(k) = \frac{R_s}{1 + iQ(k_r/k - k/k_r)}, \tag{16}$$

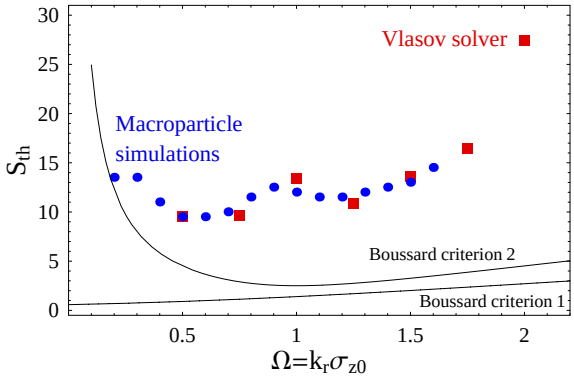

FIG. 5: The instability threshold S_{th} in terms of the dimensionless parameter S (proportional to the bunch population) for a broadband resonator as a function of $\Omega = k_r\sigma_{z0}$ for $Q = 1$ as determined numerically from macroparticle simulations (blue dots) and Vlasov solver in time domain (red squares) is compared against Boussard's criterion (solid lines) in formulation no. 1 [Eq. (20)] and no. 2 [Eq. (22)]. Results from macroparticle simulations are courtesy of S. Heifets.

corresponding to a wake potential that vanishes for $z > 0$ and for $z \leq 0$ is

$$W_{\rm res}(z) = -cR_s\frac{k_r}{Q}e^{k_r z/2Q}\left[\cos(k_1 z) + \frac{\sin(k_1 z)}{(4Q^2-1)^{1/2}}\right] \tag{17}$$

where $k_1 = k_r(1 - 1/4Q^2)^{1/2}$. Stability analysis in the presence of a broadband resonator is best carried out in terms of the scaled (dimensionless) bunch population [6]

$$S \equiv I_c\frac{\omega_0}{R_s}Q = \frac{2Nr_e}{\gamma\nu_s\sigma_{\delta 0}}\frac{k_r R_s}{QZ_0}. \tag{18}$$

The threshold of instability S_{th} depends only on the two variables Q and $\Omega = k_r\sigma_{z0}$. For $Q = 1$ the instability threshold S_{th} is shown in Fig. 5 as a function of Ω as determined from macroparticle simulations (blue dots, [8]) and the Vlasov solver used in the present study (red squares). The simulations results are contrasted to the prediction of the Boussard criterion obtained using both the above prescriptions for $[Z/n]$ (the two black curves in the picture).

Specifically from the first prescription we have

$$[\mathrm{Z/n}]_{\rm res} = \frac{R_s\sigma_{z0}}{R}\int_{-\infty}^{\infty}\frac{dte^{-t^2\Omega^2}}{\sqrt{t^2+Q^2(1-t^2)^2}} \simeq \sqrt{\pi}\frac{\sigma_{z0}}{R}\frac{R_s}{Q\Omega}, \tag{19}$$

where the approximate equality is valid for $\Omega \gtrsim 0.5$. The corresponding critical S_{th} is obtained by first inserting (19) into (14) to obtain N_{th} and then inserting $N = N_{th}$ in (18):

$$S_{th} = \frac{2N_{th}}{\gamma\nu_s\sigma_{\delta 0}}\frac{k_r R_s}{QZ_0} = \sqrt{2\pi}\frac{\sigma_{z0}}{R}\frac{R_s}{[\mathrm{Z/n}]_{\rm res}} \simeq \sqrt{2}Q\Omega. \tag{20}$$

Following the second prescription we have

$$[\mathrm{Z/n}]_{\rm res} = \frac{\sigma_{z0}}{R}\frac{R_s}{\left[1+Q^2(\Omega-\Omega^{-1})^2\right]^{1/2}}, \tag{21}$$

yielding

$$S_{th} = \sqrt{2\pi}\left[1+Q^2(\Omega-\Omega^{-1})^2\right]^{1/2} \simeq \sqrt{2\pi}Q\Omega, \tag{22}$$

with the second equality valid for large Ω.

For this resonator model of impedance Fig. 5 shows that the Boussard criterion (in both formulations) gives a considerably more pessimistic estimate of the instability threshold than the more accurate numerical simulations,

Observe that wake potential for the single resonator model is not very dissimilar from the wake potential found for the rf cavities, a leading source of machine impedance for the DRs. We can then try to fit the impedance of the resonator model against the impedance calculated numerically for a rf cavity. The result from this fit is reported in Appendix A and yields $k_r \simeq 244$ m^{-1} and $Q \simeq 0.8$. The parameter Q is not too different from $Q = 1$ used for the calculation of Fig. 5 and therefore, as an additional exercise, we can hope to relate the results shown in Fig. 5 to the numerical calculations of Fig. 4 for the impedance model with rf cavities only (green curve).

From $k_r \simeq 244$ m^{-1} and $\sigma_{z0} = 9$ mm we obtain $\Omega = k_r\sigma_{z0} \simeq 2.2$. In Fig. 5, $\Omega \simeq 2.2$ corresponds to a disagreement of about a factor $11 \sim 12$ between simulations and Boussard's criterion in formulation no. 1 (extrapolating a bit beyond the last data point reported).

By contrast, numerical solutions of the Vlasov equation show that the current threshold in the presence of the 18 rf cavities is about a factor 6 larger than the Boussard value (see end of Sec. IV).

This confirms that for wake potentials close in shape to that of a single resonator the Boussard criterion can exaggerate the impact of collective effects on beam stability by about an order of magnitude.

VI. CONCLUSIONS

Our calculations show that what we believe are the main sources of impedance for the ILC damping rings, namely the rf cavities, resistive wall and the BPMs, would be responsible for a single-bunch longitudinal instability at about $N = 100 \times 10^{10}$ part./bunch, *i.e.* a factor 50 above the design bunch population. This is still an incomplete model of impedance and, as we have warned, marginal modifications to the profile of the wake potential either due to components not yet considered or inadequacy of the models used could result in a noticeable impact on the beam dynamics. However, we argue that the safety margin is sufficiently large to allow for a revision of the choice of momentum compaction. The momentum compaction for the lattice considered here, $\alpha = 4.2 \times 10^{-4}$, was set to a fairly conservative large value in response to preliminary and very rough preliminary estimates carried out during the lattice configuration studies [2] using a value of momentum compaction three times smaller. Those estimates were inaccurate in two ways: they *i)* were based on rough models of impedance and *ii)* made use of the Boussard criterion. Indeed, one of our goals in this report was to remind ourselves that outside its legitimate range of application the Boussard criterion can yield a widely inaccurate estimate of the instability. Based on the present results it appears that a significantly smaller momentum compaction, which would be beneficial for easing the demand on the rf system in order to maintain an acceptably small bunch length, could be tolerated. Of course, due consideration to other instabilities (*e.g.* those triggered by electron cloud) will have to be given before setting new lattice specifications.

VII. ACKNOWLEDGMENTS

This work was carried out in close collaboration with the following SLAC colleagues: K. Bane, S. Heifets, Z. Li, C. Ng, A. Novokhatski, G. Stupakov, and R. Warnock. The wake potential calculations were carried out by Z. Li and C. Ng. Work supported by Department of Energy Contract No. DE-AC02-05CH11231.

APPENDIX A: APPROXIMATION OF AN RF CAVITY AS A BROAD BAND RESONATOR

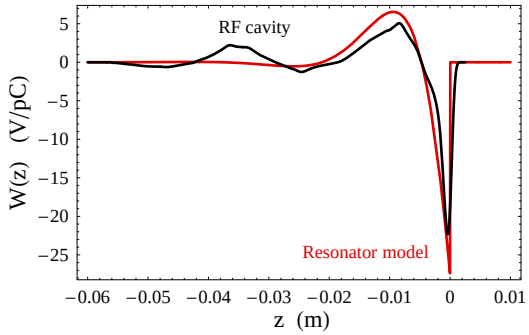

FIG. 6: Fitting of the wake potential of a road band resonator against that of a single rf cavity.

We report on an attempt to fit the parameters for the resonator impedance model against the numerical calculation of the rf cavity wake. The fitting was done 'by eye', by trying to match the most prominent features of the wake profile, black curve in Fig. 6. The broadband resonator for the wake shown in the picture (red curve) has parameters $Q = 0.8$, $k_r = 244$ m^{-1}, and $R_s = 300$ Ω. Real and imaginary parts of the impedance are compared to those of the rf wake in Fig. 7 and Fig. 8.

The [Z/n] factor evaluated for this impedance (Eq. 19) is $[\mathrm{Z/n}]_{\mathrm{res}} = 2.6$ mΩ/cavity. By contrast for the numerical rf wakes (Eq. 15) one finds: $[\mathrm{Z/n}]_{\mathrm{rf}} = 3.0$ mΩ/cavity.

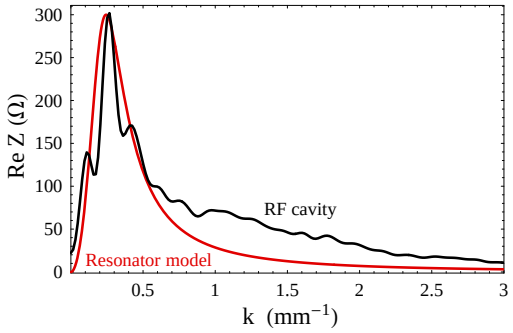

FIG. 7: Real part of the impedance for a single rf cavity and resonator model.

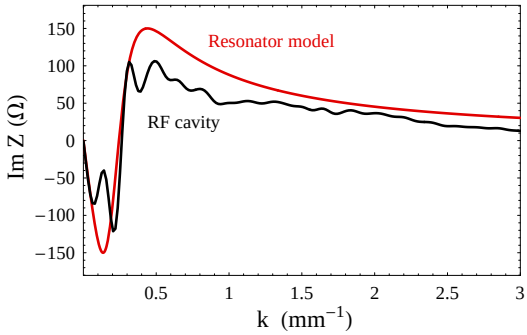

FIG. 8: Imaginary part of the impedance for a single rf cavity and resonator model.

[1] M. Venturini, K. Bane, S. Heifets, Z. Li, C. Ng, A. Novokhatski, G. Stupakov, and R. Warnock, *Impedance and single-bunch instability calculations for the ILC Damping Rings*, Proceedings of the Part. Accel. Conf. 2007, Albuquerque NM, (2007); also as LBNL Report LBNL-63107, (2007).

[2] A. Wolski, J. Gao, and S. Guiducci, *Configuration Studies and Recommendations for the ILC Damping Rings* (February 4, 2006). Lawrence Berkeley National Laboratory. Paper LBNL-59449. http://repositories.cdlib.org/lbnl/LBNL-59449.

[3] A. Chao, Physics of Collective Beam Instabilities in High Energy Accelerators, John Wiley & Sons, Inc., New York (1993).

[4] K. Bane, private communication.

[5] M. Venturini, R. Warnock, R. Ruth, and J. A. Ellison, Phys. Rev. ST Accel. Beams **8**, 014202 (2005).

[6] K. Oide and K. Yokoya, KEK Preprint 90-10 (1990).

[7] C. Ng, private communication.

[8] S. Heifets, private communication.

[9] No further work was carried out in the remainder of FY-2008 as a consequence of the budgetary changes introduced by Congress at the end of 2007. At the time of the completion of this report it is still not clear whether funding will be available for further EDR activities for the Damping Rings.

[10] Sometimes the Boussard criterion is stated in the form $[\mathrm{Z/n}]_{\mathrm{th}} = \frac{Z_0}{N}\sqrt{\frac{\pi}{2}}\frac{\gamma\eta\sigma_{\delta 0}^2\sigma_{z0}}{r_e}$, where N is the nominal bunch population and $[\mathrm{Z/n}]_{\mathrm{th}}$ is the maximum allowable machine impedance to avoid instability. For the present design of the DR lattices $[\mathrm{Z/n}]_{\mathrm{th}} = 508$ mΩ.